Journal of Drug Delivery Science and Technology 99 (2024) 105940

Contents lists available at ScienceDirect

Journal of Drug Delivery Science and Technology

journal homepage: www.elsevier.com/locate/jddst

Electrospun amygdalin and *Inula helenium* extract-loaded polylactic acid (PLA)/Polyvinylpyrrolidone (PVP) nanofibrous patches for colon cancer treatment: Fabrication, characterization and antitumour effect results

Rabia Betul Sulutas [a,b], Sumeyye Cesur [a,b,*], Serap Ayaz Seyhan [a,c], Dilek Bilgic Alkaya [a,c], Ali Sahin [d], Nazmi Ekren [a,e], Oguzhan Gunduz [a,b]

[a] Center for Nanotechnology & Biomaterials Application and Research (NBUAM), Marmara University, Turkey
[b] Department of Metallurgical and Materials Engineering, Faculty of Technology, Marmara University, Turkey
[c] Department of Analytical Chemistry, Faculty of Pharmacy, Marmara University, Istanbul, Turkey
[d] Department of Biochemistry, School of Medicine/Genetic and Metabolic Diseases Research and Investigation Center, Marmara University, Istanbul, Turkey
[e] Department of Electrical and Electronical Engineering, Faculty of Technology, Marmara University, Turkey

ARTICLE INFO

Keywords:
Colon cancer
Plant extract
Amygdalin
Nanofibrous patch
PLA
PVP

ABSTRACT

In this study, 75PLA/25PVP nanofibrous loaded with amygdalin (AMG) and *Inula helenium* (*I.H*) extract were produced by electrospinning method in order to prevent local colon cancer recurrence, and the effect of the produced nanofibrous on the HCT-116 cell line was examined in vitro. When the scanning electron microscopy (SEM) images were examined, the fiber diameter of the 75PLA/25PVP group was measured as 443.74 ± 79 nm, but the addition of *I.H* and AMG caused a thickening effect on the fiber diameters. Drug release results show the controlled release period of 75PLA/25PVP/*I.H* and 75PLA/25PVP/AMG loaded nanofibrous patches within 180 h. Slowly degrading nanofibrous remained durable for up to 25 days. When the in vitro cytotoxicity results were analyzed, all nanofibrous were found to be effective in inducing cytotoxicity against HCT-116 colon cancer cells. The most effective group is the group in which *I.H* extract and AMG drug are loaded onto the nanofibrous together. AMG drug and *I.H* plant extract showed effects on the colon cancer cell line in in vitro experiments. Considering all the results I.H and AMG loaded nanofibrous can be implanted into solid tumor cells in order to reduce the risk of local recurrence of cancer after surgery in colon cancer.

1. Introduction

Lung cancer, breast cancer, and colon cancer are the most common types of cancer [1]. The incidence of colon cancer has increased rapidly since 1975, with approximately 300,000 new cases and 200,000 deaths each year in Europe and the United States. The stage of colon cancer affects the long-term survival of this disease process. Surgery is a therapeutic method after early diagnosis and detection. Colon cancer metastases develop in at least 40 % of patients, and therefore, the prognosis of colon cancer is poor [2,3]. Surgery, chemotherapy, and radiotherapy are the main strategies used for the treatment of colon cancer. 5-fluorouracil (5-FU), a cytotoxic chemotherapy drug used by intravenous injection for the last 40 years, shows low efficacy. Despite its high toxicity and low efficacy, 5-FU remains the most valid chemotherapy drug in colon cancer treatments. Although the chemotherapy method offers limited and temporary methods, it has aggressive side effects. Many of the patients treated with these methods also develop drug resistance, which causes the progression of the disease [4]. The use of plant-derived drugs in the field of oncology (*Catharanthus roseus*, *Podophyllum peltatum* L., *Taxus brevifolia* Nutt., *Taxus baccata*, etc.) is considered as a complementary alternative option in oncology. In this way, new cytotoxic compounds are isolated every year due to plants adopted as complementary and alternative options. These cytotoxic compounds, which can be obtained from many plants, can provide new opportunities for cancer treatments [5,6].

Plant-derived drugs were essential in cancer treatments in phytomedicine history because they had low toxicity and high efficacy. Medicinal plants containing many natural active ingredients are known as potential anticancer agents [7]. In particular, according to recent studies, it has been revealed that products with natural phytochemical

* Corresponding author. Center for Nanotechnology & Biomaterials Application and Research (NBUAM), Marmara University, Turkey.
E-mail address: sumeyye.cesur@marmara.edu.tr (S. Cesur).

https://doi.org/10.1016/j.jddst.2024.105940
Received 3 January 2024; Received in revised form 28 June 2024; Accepted 3 July 2024
Available online 4 July 2024

components are an alternative cancer treatment method due to their anti-cancer properties [8]. Alantolactone, a sesquiterpene lactone found in the literature as "*Elecampane*" in Latin, is an active component of the Chinese herbal medicine *Inula helenium* (*I.H)* [9]. Sesquiterpene lactones, especially alantolactone and isoalantolactone, which are abundant in this plant, have been shown to have anticancer properties. These properties include preventing drug resistance and metastasis and stimulating apoptosis [10].

The natural substance found in amygdalin (D-mandelonitrile-b-D-glucoside-6-b-glucoside) is an anticancer agent, belongs to the cyanogenic glycoside family and is a chemical compound obtained from the seeds of fruits such as apricots, cherries, almonds, lima beans and peaches [11,12]. AMG is a substance with antitumour properties [13]. In addition to its antitumour properties, AMG has antioxidant, antibacterial, and anti-inflammatory properties. Amygdalin, which is non-toxic when taken orally, also has immunomodulating properties [14]. AMG has also been found to reduce the expression of cell cycle-related genes in human colon cancer cells. Park et al. observed changes in gene expression in SNU-C4 cells after AMG treatment. They found that AMG was associated with the cell cycle-associated genes ATP-binding cassette, exonuclease 1 (EXO1), topoisomerase (DNA) I (TOP1), and found to down-regulate subfamilies F [15].

Scale fibers can be produced using electrospinning. While producing nanofibrous patches, the electrophysical interaction between the electrostatic force and the polymer solution at the needle tip is the basic mechanism. The pores of the nanofibrous patch and the homogeneous surface area of the nanofibrous patch also promote cell attachment and growth [16]. Due to their nanoscale fiber diameter, high porosity, and substantial surface area, electrospun nanofibrous patches have a wide range of applications in the biomedical field, including tissue engineering scaffolds, wound dressings, and drug delivery systems. Numerous advantages of the electrospinning technique include its simplicity, cost-effectiveness, scalability, capacity to incorporate a high drug loading in the polymer solution, and adaptability to spinning various polymeric fibers. Since the drug release profile from electrospun nanofibrous patches can be easily adjusted to the target site and the drug delivery profile can be controlled by modulating the fiber composition, porosity, and morphology, electrospun nanofibrous patches have also been used to carry anti-cancer drugs [17].

Due to its advantages in research for electrospin technology, such as biocompatibility, high mechanical strength, affordability, eco-friendliness and compatibility with drug delivery systems, polylactic acid (PLA) is usually chosen [18]. A biodegradable synthetic material called PLA is appropriate for various tissue engineering applications [19]. It was discovered that by removing the initial burst, PLA-based nanofibrous patches could produce the desired release kinetics of the active ingredients [20]. Polyvinylpyrrolidone (PVP) is non-toxic and biocompatible as an essential synthetic material [21]. PVP has high hydrophilicity, thermal stability, tensile strength, solubility, bendability, and film-forming properties. Therefore, PVP can be considered a promising bioengineering material in medical applications [22].

This study examined the therapeutic effect of layered nanofibrous patch cover produced by electrospinning method and combinations of two active ingredients on colon cancer cells. In this study, an electrospun fiber patch sheath was produced and characterized to examine the therapeutic effect of two active ingredients on colon cancer cells. The behavior of *I.H* and AMG-loaded nanofibrous patches against HCT-116 colon cancer cells was examined. The innovative aspect of this study is that a plant extract with anti-tumor effect and drug were combined in the same nanofibrous patch and the loading results were compared together and separately. This study is promising in terms of developing tissue engineering applications to create a different perspective and solution for the use of biocompatible polymer-based electrospun nanofibrous patches in post-cancer surgery treatments.

2. Materials and methods

2.1. Materials

Poly (L-lactic acid) (PLA) 2003D was purchased from Nature Works LLC, Minnetonka, MN, Poly (vinylpyrrolidone) (PVP) with Mw of about 40.000 was purchased from Sigma-Aldrich, Chloroform, Ethanol, Dimethyl sulfoxide (DMSO), Tween 80 (viscous liquid), Amygdalin, phosphate-buffered saline (PBS) pH 7.4 solution were purchased from Sigma-Aldrich. HCT-116 Cell Line Human, DMEM high glucose with 4.5 g/L D-glucose was bought from Sigma-Aldrich (St. Louis, MO).

2.2. Methods

2.2.1. Preparation of plant extract

The leaf parts of *I.H* plant were collected. The extraction procedure was described by Alkaya et al., 2019 [23]. The material was first dried and ground in a blender until it became a fine powder. Then, 2 g of *I.H*, pulverised, was extracted in an ultrasonic extraction device containing 70 % ethanol at 60 °C for 1 h and with 3 consecutive extractions. The extract was first filtered through Whatman blue band filter paper and then evaporated under reduced pressure in the evaporator at 50 °C until the moisture dried. The residue obtained after drying was weighed as crude extract and transferred to bottles. It was kept tightly closed under appropriate storage conditions at +4 °C and in a dark environment. The crude extract was dissolved in DMSO for use in nanofibrous patch production.

2.2.2. Preparation of electrospun solutions

To prepare the solution containing *I.H.,* 9ml *of chloroform and 0.8 g of PLA were* mixed at 500 rpm without heat. Later, 1 wt% Tween 80 was added dropwise to the PLA solution, and the solution was stirred for 20 min at 350 rpm. In a separate beaker, 40 mg of *I.H* in powder form in 1 ml of DMSO was added and mixed for 5 h at 350 rpm without heat. Chloroform/PLA solution and DMSO/*I.H* solution were mixed. For the second solution, 1 g of PVP and 10 ml of ethanol were mixed in a separate beaker without heat. 40 mg of AMG drug was added to the dissolved solution. This polymer combination was mixed in proportions of 75:25, 50:50, and 25:75 percent. 7.5 ml of PLA-containing solution and 2.5 ml of PVP-containing solution prepared in each group were mixed. The solution containing 75 % Chloroform/PLA and 25 % Ethanol/PVP was the ratio that gave the best results. Because SEM results were compared as a result of 3 different ratios (75:25, 50:50, 25:75) tried and it was observed that the ratio with the best, smoothest and most homogeneous nanofibrous fiber morphology was the 75:25 (75PLA/25PVP) solution. There are 5 groups. 75PLA/25PVP is a non-drug-loaded group. 75PLA/25PVP/*I.H* is *I.H* loaded group and 75PLA/25PVP/AMG is AMG loaded group. 75PLA/25PVP/*I.H*/AMG/(B) is a group of solutions in which 75 % *I.H* and 25 % AMG are blended (B). 75PLA/25PVP/*I.H*/AMG (DL) is a group of solutions in which 75 % *I.H* and 25 % AMG are double layer (DL). It is formed by overlapping the first layer of AMG-loaded fiber and the second layer of *I.H*-loaded fiber. It is a single fiber patch with two double layers (Fig. 1).

2.2.3. Electrospinning of nanofibrous patch

A laboratory-type device (NS24, Inovenso Co., Turkey) was used for electrospinning. The prepared solutions were transferred to the injector. The injector was connected to a pump where the flow rate was adjusted. The injector in the pump was connected to the needle of the electrospinning machine with the help of a polyethylene plastic cable. The distance between the needle and the collecting metal cylinder is 12 cm. Parchment paper was wrapped around the collector metal cylinder. All solution groups were applied at 0.7 ml/h and 29 kVa.

2.2.4. Scanning electron microscopy (SEM)

SEM (EVO LS 10, ZEISS) device was used to display the morphologies

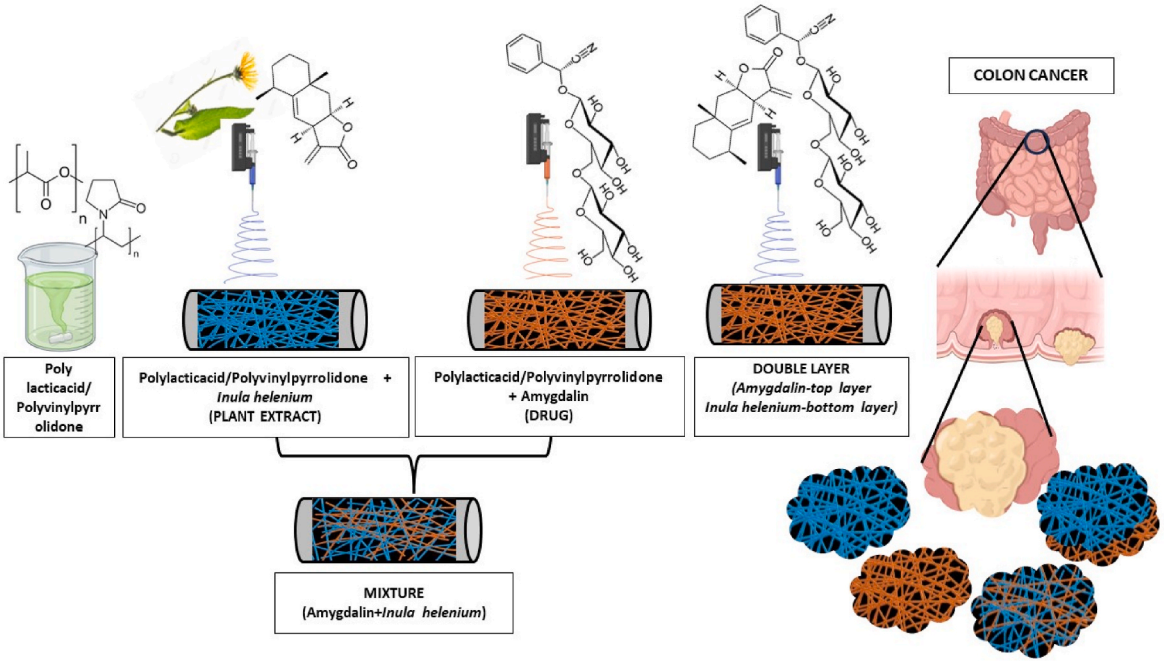

Fig. 1. Schematic representation of the polymer combination used for the solution and the produced electrospun nanofibrous.

of 5 groups consisting of pure, *I.H,* and AMG-loaded nanofibrous patches. The samples were cut, and their surfaces were gold-palladium coated for 120 s with Quorum SC762 Mini Sputter Coater. On the obtained SEM images, 100 diameter measurements were taken from the nanofibrous patch with nm adjustment for each group. (Olympus AnalysisSIS, USA). According to the data, histogram graphs were drawn, and the average diameter size information was obtained.

2.2.5. *Fourier transform infrared spectroscopy (FT-IR)*

FTIR device (Jasco FT/IR-4700) was used to analyse bond structures in the functional groups of nanofibrous patches. For this analysis, all spectra were analyzed and evaluated at a scan range of 4000 cm^{-1} to 400 cm^{-1}, at a scan rate of 32, and at a resolution of 4 cm^{-1}.

2.2.6. *Differential scanning calorimetry (DSC)*

A differential scanning calorimetry (DSC) device (Shimadzu, Japan) was used to determine the main thermal transitions and heating movements, such as glass transition temperature (Tg) and melting temperature (Tm). Adjustment was made for the nanofibrous patch at a heating rate of 10 °C/min, with a temperature range of between 25 °C and 300 °C.

2.2.7. *High-Performance Liquid Chromatography (HPLC) phenolic substance analysis*

HPLC method (High-Performance Liquid Chromatography) was used to determine phenolic substances. Phenolic compounds were detected at a wavelength of 278 nm and a flow rate of 0.8 mL/min. An Agilent Eclipse XDB C-18 (250 × 4.6 mm) 5 μm reverse phase column was used. The column temperature is 30 °C. Separation was done by applying a gradient program with a binary solver system. Solution A is 3 % acetic acid; solution B is methanol. The HPLC device used in the study is Shimadzu (Kyoto, Japan) brand and includes the Shimadzu brand detector (SPD-M10A vp Photo Diode Array detector), column oven (CTO-10A vp), pump (LC-10AD vp), degasser (DGU-14A).) and automatic injection (SIL-10AD vp) system. In the High-Performance Liquid Chromatography (HPLC) method, the column used is an essential component of liquid chromatography and has a significant impact on the quality and precision of analytical separation. The column selection is based on the characteristics of the analytes, the purpose of the analysis, and other experimental conditions. The type of column we preferred in this study is the Agilent Eclipse XDB C-18, a liquid chromatography column with dimensions of 250x4.6 mm. The column has a length of 250 mm and an inner diameter of 4.6 mm. It features a particle size of 5 μm, which is a crucial factor influencing the chromatographic resolution. The designation C-18 defines the chemical surface of the column. This column is typically used to separate analytes based on hydrophobic interactions. C-18 refers to an alkyl ligand with a carbon chain length of 18.

2.2.8. *Mechanical properties*

A tensile test was applied to measure the mechanical strength of the nanofibrous patch with a tensile testing machine (Shimadzu Corporation, EZ-LX, Kyoto, Japan). Before testing, nanofibrous patches were cut to 10 × 50 mm size. Each cut sample was subjected to thickness measurement with the help of a digital micrometre (Mitutoyo MTI Corp., ABD). The average thickness values were recorded in the computer program together with the name information before the test started and the tensile test was started. This test was repeated three times for each group for consistency.

2.2.9. *Swelling and degradations*

In nanofibrous patch samples, swelling, and degradation test was performed for all groups to determine the water uptake and the change in mass over time. For the swelling test, three nanofibrous patch pieces of equal weight were prepared from each group in 1 ml tubes using phosphate-buffered saline (PBS) with a pH value of 7.4. 1 ml of PBS and fiber fragments kept in Eppendorf tubes were kept in a thermal shaker (BIOSAN TS-100) at 37 °C for 24 h, and at the end of 24 h, the samples were removed from the PBS liquid and weighed (W_w) on an electronic balance. Equation (1) measured the swelling value [24].

$$SD = \frac{W_w - W_0}{W_0} \cdot 100 \qquad \text{Equation (1)}$$

Nanofibrous patches were cut equally for each group and weighed for the degradation process. Weighed nanofibrous patches were kept in an Eppendorf thermal shaker containing 1 ml of PBS for 24 h at 37 °C. After 24 h, the fibers and PBS were separated from each other. This nanofibrous patch was placed inside the empty Eppendorf, and the Eppendorf were dried in a thermal heater at 37° for 24 h with the lids

open. After 24 h, the dried fiber sample weights (W_t) were measured on an electronic balance and the results were recorded according to Equation (2) [25].

$$D = \frac{W_0 - W_t}{W_0} \cdot 100 \quad \text{Equation (2)}$$

2.2.10. In vitro drug release

For in vitro drug release of *I.H* and AMG-loaded nanofibrous patch, 5 mg nanofibrous patch were cut from each group and transferred to Eppendorf tubes containing 1 ml PBS. Measurements of 15 min, 30 min, 1 h, 2 h, 3 h, 4 h, 6 h, 8 h, 12 h, 24 h, 48 h, and 72 h were measured with a UV spectrophotometer (Shimadzu UV-3600, Kyoto, Japan) between 190 nm and 550 nm. PBS (pH 7.4) in Eppendorf was refreshed for the measurement of each hour. As a result of the measures, drug release graphs were drawn. In the spectrum graph obtained from the measurement made between 190 nm and 550 nm wavelengths, AMG drug reached its maximum absorption value at 210 nm. It reached *I.H* max absorption value at 240 nm.

2.2.11. Cell culture test and MTT cytotoxicity assay

Material sterilisation was performed using a Class II Laminar flow cabinet. For sterilisation, the materials were kept under UV light for 90 min. For optimization of scaffold microenvironment, the scaffolds were incubated in 20 μL of growth medium (DMEM with 10 % FBS and 1 % penicillin/streptomycin) for 1h at 37 °C in humid 5 % CO_2 incubator in a 96-well plate were used to stabilise the materials. $5x10^3$ HCT-116 cells were seeded onto the materials in the 96 well plates like on standard cell seeding procedure. At the same time, monolayer cell cultures were incubated with same number of cells in 150 μl as a control. The cell-materials constructs and monolayer cultures were incubated at 37 °C, 5 % CO_2 for 1, 3 and 7 days in humidified incubator (NuAire). An MTT (3-(4, 5-dimethylthiazolyl-2)-2, 5-diphenyltetrazolium bromide) (Glentham Life Sciences) test was performed at 1,3, and 7-day incubation periods to analyse cell viability in nanofibrous patches. 5 mg/mL MTT solution was added according to manufacturer's protocol and incubated for 5 h at 37 °C with 5 % CO_2. Than, 0.1 mL of dimethylsulfoxide (DMSO) was added. Plates were reincubated (15 min at 37 °C and 5 % CO_2) to observe cell viability. Absorbance was measured using a microplate reader (Enspire, PerkinElmer) at a wavelength of 560 nm.

Cell viability was calculated according to this formula

$$: \frac{Sample - Positive\ Control}{Negative\ Control - Positive\ Control}.100$$

2.2.12. DAPI staining

The DAPI staining method was applied to investigate the adhesion of colon cancer cells to AMG and *I.H* loaded nanofibrous patches and cell viability. Colon cancer cells at 10^5 cells/mL density were seeded on each sterilised nanofibrous patch in a 96-well plate and cultured in a medium containing DMEM at 37 °C under 5 % CO for 1, 3, and 7 days. At the end of the incubation, the samples were fixed with 4 % Formaldehyde for 20 min. Then, it was permeabilised with 0.1 % TritonX solution for 15 min and washed with PBS. Cell nuclei were stained with 1 μg/ml DAPI solution for 5 min in the dark. The nanofibrous patches were then rinsed three times with PBS to remove excess DAPI and examined using a fluorescence (Leica) microscope.

2.2.13. SEM analysis

Colon cancer cell growth and spread morphology on the nanofibrous patch were investigated with scanning electron microscope (SEM) observation. AMG and *I.H* loaded nanofibrous patches were washed twice with PBS; they were fixed in 2.5 % glutaraldehyde solution for 24 h at 4 °C. The excess glutaraldehyde was then removed by washing with PBS, and nanofibrous patches were dehydrated in a graded ethanol series. The samples were sputter-coated with gold and examined using SEM (EVO MA-10, Zeiss).

2.2.14. Statistical analysis

A single-factor ANOVA analysis program was used. The SPSS analysis program was used for the diameter measurement of the nanofibrous patch. In evaluating all results, they are given as mean ± STD. Statistical significance was defined as $p < 0.05$.

3. Result and discussion

3.1. Morphological characterization of nanofibrous patches

For the diameter and morphological analysis of the produced nanofibrous patch, the diameter of 100 fibers from each group was measured. The histogram graph made according to these measurements is shown in Fig. 2. The diameters of the obtained fibers were measured as 443.74 ± 79 nm for the pure group as 75PLA/25 PVP. It was estimated at 525.34 ± 87 nm for the group with only *I.H* added as 75PLA/25PCP/*I.H*. It was measured at 536.95 ± 140 nm for the only AMG-added group 75PLA/25PVP/AMG. The group is 75PLA/25PVP/*I.H*/AMG (B), in which *I.H* and AMG active ingredients were blended and added together, measured as 494.21 ± 100 nm. The group is 75PLA/25PVP/*I.H*/AMG (DL), in which *I.H* and AMG active ingredients were made separately, without mixing, as a double layer was measured at 501.38 ± 93 nm. According to the results, the pure group has the smallest diameter measure. The effect of AMG active ingredient on increasing the diameter measurement is higher than *I.H*. The fiber diameters were measured thicker in the groups in which the active ingredients were added separately. When *I.H* and AMG were mixed and loaded into the fiber, the fiber diameter decreased compared to when loaded independently. Sridhar et al., in their study on cancer, observed an increase in nanofibrous diameter when they added the active ingredients of turmeric and aloe vera to PCL, a synthetic polymer such as PLA [26]. In the nanofibrous wound dressing study by Fan and Daniels, the fiber diameters obtained by loading the triterpene extract from the birch plant into PLA are compared. It is observed that the fiber loaded with triterpene extract has a thinner diameter than the triterpene-free fiber. There are studies in the literature that support the plant extract to increase or decrease the diameter thickness or not cause any change [27].

3.2. Chemical properties of the nanofibrous patches

FT-IR analysis was performed to investigate the functional groups of the nanofibrous patch as well as the interactions between the components. The molecular structures of pure PLA, PVP, *I.H,* and AMG and all nanofibrous patch samples that separate, blend, and double layers produced by electrospinning methods are given in Fig. 3A and B. The primary characteristic absorption bands are C═O vibration peak at 1750 cm^{-1}, CH_3 asymmetric shear at 1456 cm^{-1}, CH_3 and C–H bending vibrations at 1386 cm^{-1} and 1358 cm^{-1}, C–O–C stretching vibration at 1265 cm^{-1}, C–O–C stretching at 1080 cm^{-1}, C–CH_3 stretching, OH bending at 950 cm^{-1} and C–COO stretching at 873 cm^{-1} for pure PLA in Fig. 3A(a) respectively [28]. FTIR spectra show a band about 1017 cm^{-1} assigned to the CH_2 rocking of PVP in Fig. 3A(b). While a peak of about 1268.65 cm^{-1} referred to the twisting of CH_2 of PVP. The peak of about 1284.36 cm-1 indicated C–N stretching or C–O stretching, and the band of about 1650.77 cm-1 was assigned to the C═O stretching of the PVP [29]. Vibration bands of the AMG in Fig. 3A(c) component in the FTIR spectrum are 1620 cm^{-1} and 1455 cm^{-1} (aromatic C═C stretch), 2885 cm^{-1} (aliphatic C–H stretch), and 2932 cm^{-1} (aromatic C–H stretch). The peak showing the OH stretch is 3367 cm^{-1} [30]. The FT-IR spectrum of *I.H* in Fig. 3A(d) shows a broad peak at 3402.11 cm^{-1} and a weak one at 2923.56 cm^{-1}, showing the O–H stretching vibration and C–H stretching vibration of the CH_2 groups and marked the absorption peak. Absorption of water is shown as 1751.05 cm^{-1}, and C–H vibration to the absorption band at 1592.91 cm^{-1} is determined. Due to the C–*O*–C ring

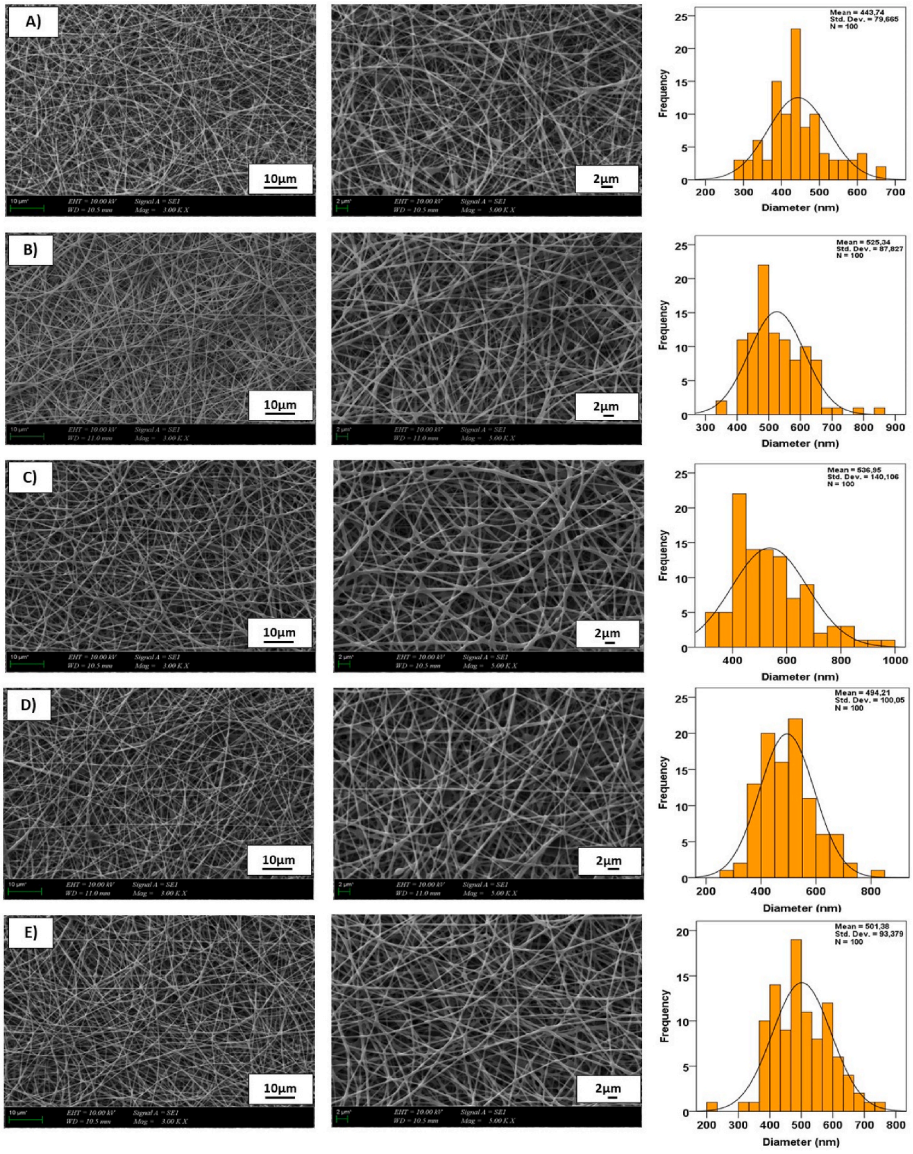

Fig. 2. Scanning electron microscopy images of nanofibrous patches; 75PLA/25PVP (A), 75PLA/25PVP/*I.H* (B), 75PLA/25PVP/AMG (C), 75PLA/25PVP/*I.H*/AMG (B) (D), and 75PLA/25PVP/*I.H*/AMG (DL) (E).

stretching vibrations and C–O stretching vibrations, the 1035.59 cm^{-1} and 981.59 cm^{-1} points are the absorption peaks. Two absorption bands at 860.10 cm^{-1} and 819.60 cm^{-1} indicate the presence of β-type glycosidic linkage and the sugar 2-ketofuranose [31]. Similar peaks with different intensities were obtained in the FT-IR spectra for the AMG and *I.H* loaded nanofibrous patch in Fig. 3B(h). According to these results, it can be said that the formulation and encapsulation were successful.

3.3. Thermal properties of nanofibrous patches

The peak lines in the DSC graph are used to examine the structural responses of the produced fibers to temperature as glass transition temperature (Tg) and melting temperature (Tm) in Fig. 3C. DSC thermograms of 75PLA/25PVP, 75PLA/25PVP/*I.H*, 75PLA/25PVP/AMG, 75PLA/25PVP/*I.H*/AMG (B) and 75PLA/25PVP/*I.H*/AMG (DL) electrospinning fibers are shown in Fig. 3C. The glass transition temperatures of the nanofibrous patch are as follows, respectively: 52.09 °C, 53.32 °C, 55.89 °C, 55.96 °C, 55.27 °C. When *I.H* was added alone, it slightly increased the glass transition temperature of the 75PLA/25PVP nanofibrous. A similar increase was observed when the AMG drug was added alone. It was observed that the glass transition temperature increased more when the two active substances were used together. These heat values of nanofibrous patches with a single glass transition temperature peak and the absence of phase separation may be due to dispersions and interactions between polymers [28]. Melting points, respectively, are as follows, with a slight decrease: 156.73 °C, 155.32 °C, 154.75 °C, 155.65 °C, 155.45 °C. In the study conducted by Cam et al., when the thermal behaviour of progesterone P4, a steroid hormone added to the intravaginal nanofibrous patch, was examined, it was determined that the P4 hormone added to pure PLA reduced the Tm value. It has been stated that this is because PLA crystallinity is suppressed by the P4 progesterone hormone through the intermolecular interaction [32]. Similarly, when AMG and *I.H* adducts were added, the melting temperature in the pure group 75PLA/25PVP may have decreased slightly due to intermolecular interaction (see Table 1).

3.4. High-Performance Liquid Chromatography (HPLC) phenolic substance analysis

HPLC analysis was performed to determine the phenolic components

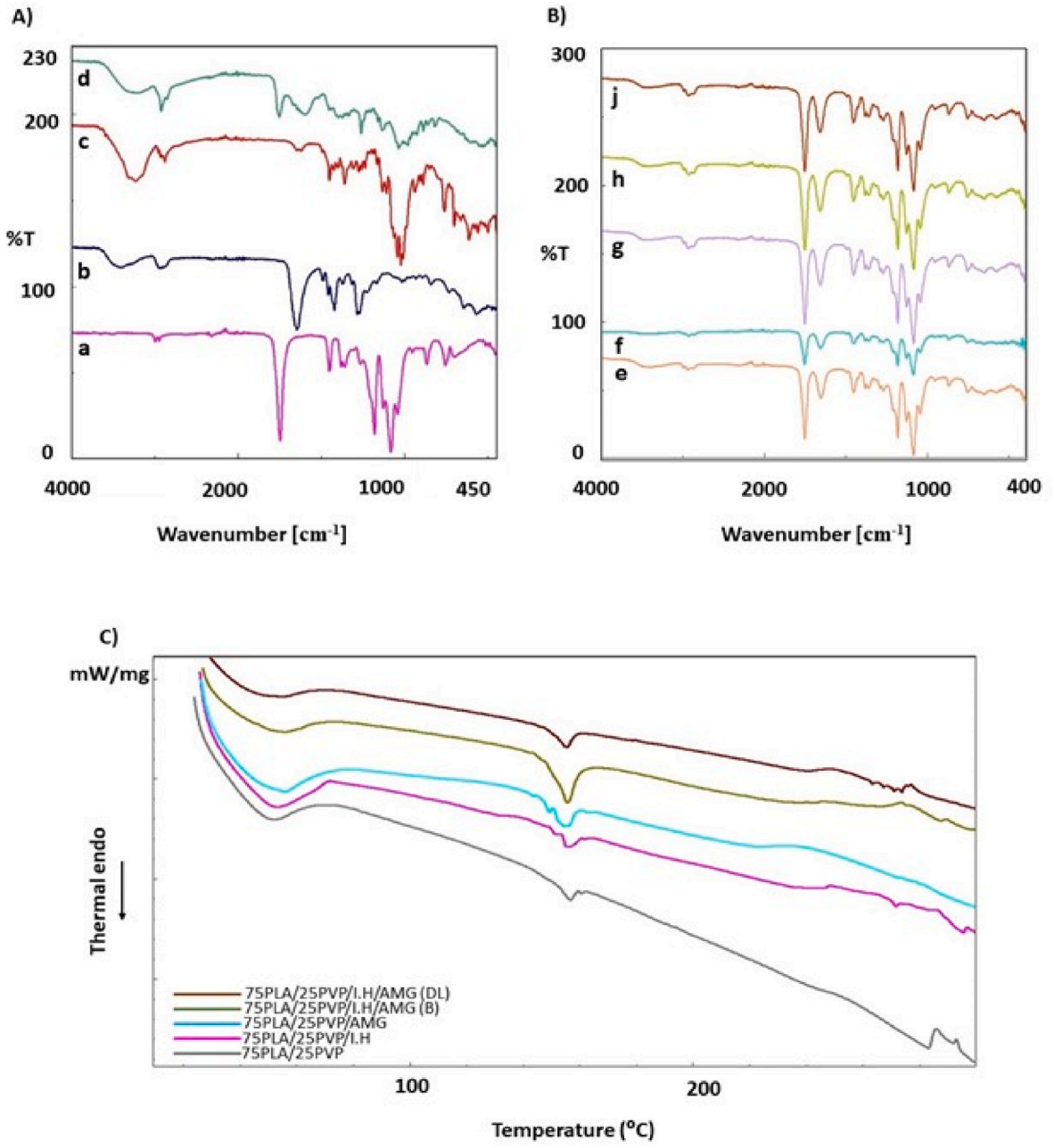

Fig. 3. FT-IR spectra of nanofibrous patch (A); pure PLA (a), pure PVP (b), pure AMG (c), pure *I.H* (d), (B) 75PLA/25PVP (e), 75PLA/25PVP/*I.H* (f), 75PLA/25PVP/AMG (g), 75PLA/25PVP/*I.H*/AMG (B) (h), and 75PLA/25PVP/*I.H*/AMG (DL) (j) (B); DSC plot showing the thermal behavior of nanofibrous patch (C).

of *I.H* extract, and the analysis results were defined as stated in Table 2. *I.H* extract used in powder form has 5 phenolic acid contents, which are the most noticeable in the chromatogram. These phenolic acids are chlorogenic acid 12205.9 μg/g, routine 1353.1 μg/g, quercetin 80.7 μg/g, cinnamic acid 19 μg/g and *p*-coumaric acid 11 μg/g, respectively in

Table 1
Components of the produced nanofibrous patch and proportions of the materials used.

	PLA	PVP	Tween 80	*I.H*	AMG
75PLA/25PVP	8 %	1 %	1 %	0	0
75PLA/25PVP/*I.H*	8 %	1 %	1 %	0.4 %	0
75PLA/25PVP/AMG	8 %	1 %	1 %	0	0.4 %
75PLA/25PVP/*I.H*/AMG (B)	8 %	1 %	1 %	0.4 %	0.4 %
75PLA/25PVP/*I.H*/AMG (DL)	8 %	1 %	1 %	0.4 %	1.4 %

Table 2
Gradient program for solutions A and B.

Time (min)	A(%)	B(%)
0	93	7
20	72	28
28	75	25
35	70	30
50	70	30
60	67	33
62	58	42
70	50	50
73	30	70
75	20	80
80	0	100
81	93	7

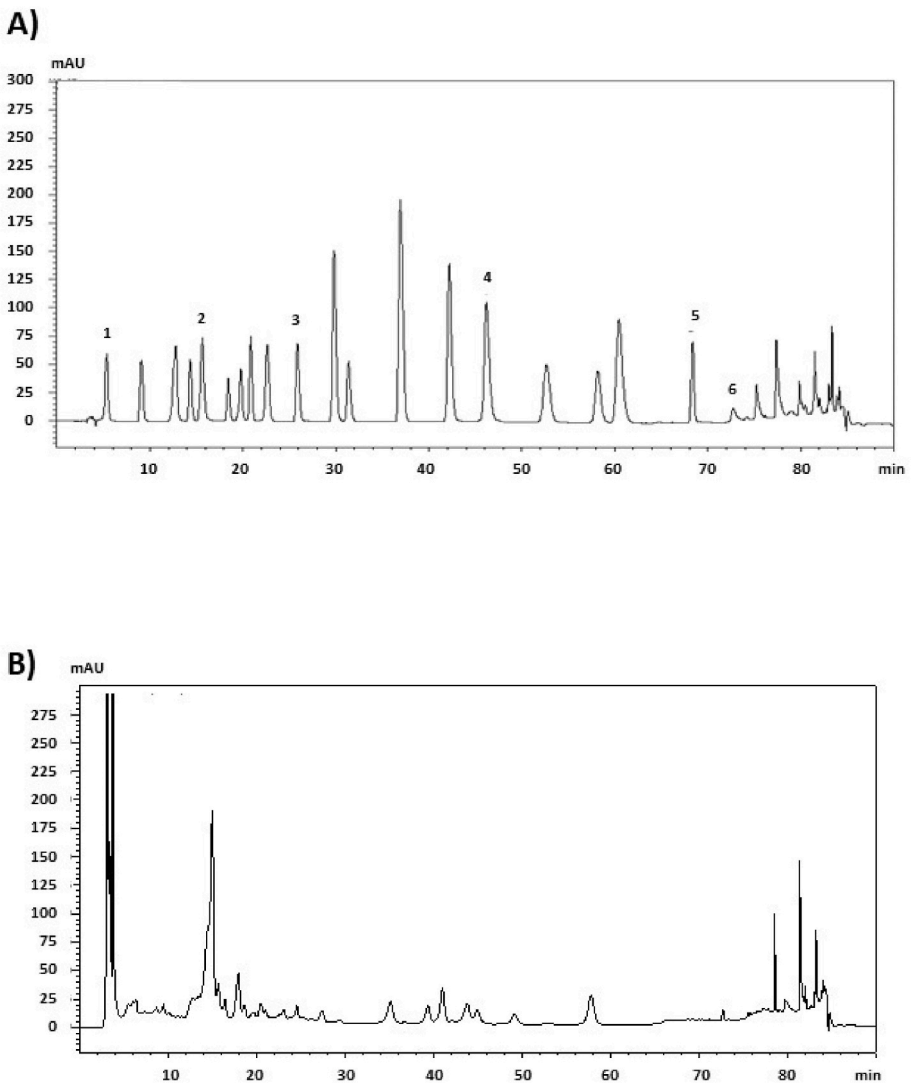

Fig. 4. HPLC chromatograms of standards and extract at 278 nm. Peak 1: gallic acid, peak 2 chlorogenic acid, peak 3: *p*-coumaric acid, peak 4: rutin, peak 5: cinnamic acid and peak 6: quercetin (A) and Chromatogram peaks of *I.H* (B).

Fig. 4B. A study conducted by Aybastıer on the DNA repair mechanism detected the presence of chlorogenic acid in the HPLC results obtained from the *I.H* plant and received data parallel to the results of our study [33]. In their article, Petkova et al. examined the extract of the *I.H* plant to obtain a high antioxidant effect. They concluded that the chlorogenic acid phenolic component was the most abundant component. Due to its rich content of phytochemicals, *I.H* is officially listed in some European pharmacopoeias. The herb roots contain lactones, thymol derivatives, triterpenes, sterol, phenolic acids and flavonoids [34,35]. Among these phenolic compounds, the five main components with anticancer activity, quercetin, routine, cinnamic acid, chlorogenic acid and *p*-coumeric acid, were measured using the regression equations of the calibration curves.

3.5. Mechanical properties of nanofibrous patches

The tensile strength (MPa) and strain at break (%) test results of five different models produced for the treatment of colon cancer are as in Fig. 5. The tensile strength value of the pure group consisting of 75PLA/25PVP polymers combination is 3581 ± 0.594 MPa. The tensile strength of the *I.H*-loaded group named 75PLA/25PVP/*I.H* decreased slightly to 3495 ± 0.969 MPa. The amygdalin-loaded fiber that was called 75PLA/25PVP/AMG dropped more sharply, measuring 2833 ± 0.547 MPa. The tensile strength of the nanofibrous named 75PLA/25PVP/*I.H*/AMG (B), in which *I.H* and AMG were mixed and loaded together, decreased slightly and was 2.449 ± 1.141 MPa. The tensile strength of the nanofibrous scaffold that is named 75PLA/25PVP/*I.H*/AMG (DL), where two active substances are produced as separate layers, is 1.508 ± 0.784 MPa. Adding active substances to the polymer affected the stretching of the produced nanofibrous. The study conducted by Stoyanova et al. shows that the plant extract added to PLA nanofibrous reduces the mechanical properties due to its strong antioxidant activity. The reason for this may be that the low molecular weight compound is mixed into the PLA matrix [36]The strain at break (%) test results are as follows, respectively: 16.028 ± 5.928, 9.633 ± 1.179, 9.069 ± 1.830, 9.715 ± 2.52, 8.056 ± 7.970; 75PLA/25PVP, 75PLA/25PVP/*I.H*, 75PLA/25PVP/AMG, 75PLA/25PVP/*I.H*/AMG (B), and 75PLA/25PVP/*I.H*/AMG (DL). According to the results, even though the breaking strain is the lowest, the group is the fiber group produced with double layers. Cesur et al. supported the findings in their article study that drug additives reduce the mechanical strength of the fiber in double-layer production [37].

3.6. Swelling and degredations

Swelling is important for biomaterials as they have effects such as

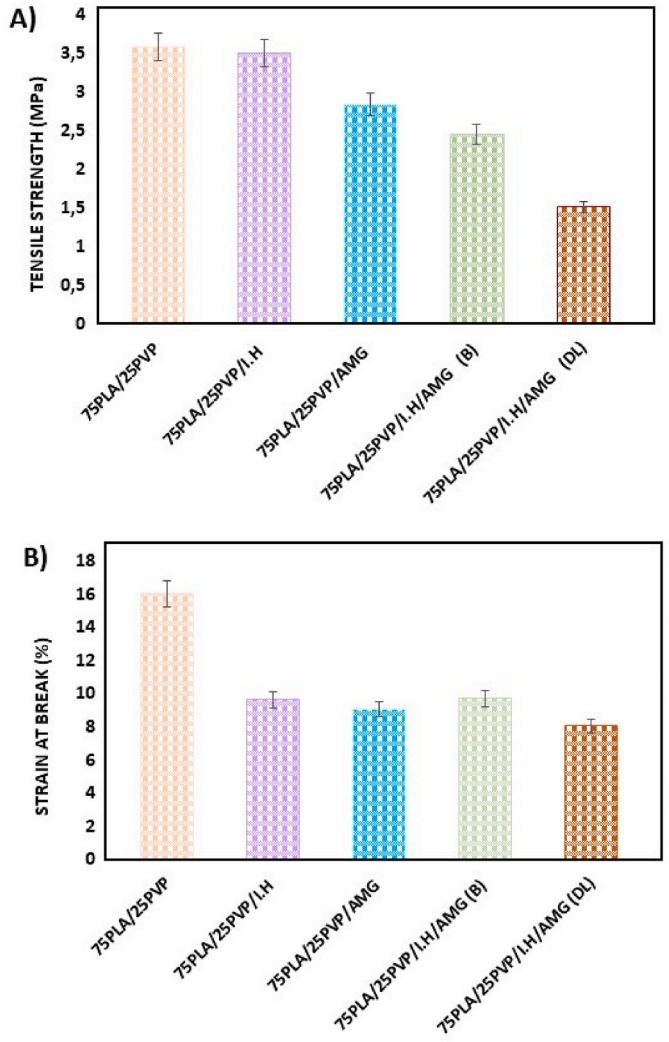

Fig. 5. Graph of tensile test measurements of electrospin nanofibrous patch: (A) tensile strength and (B) strain at break.

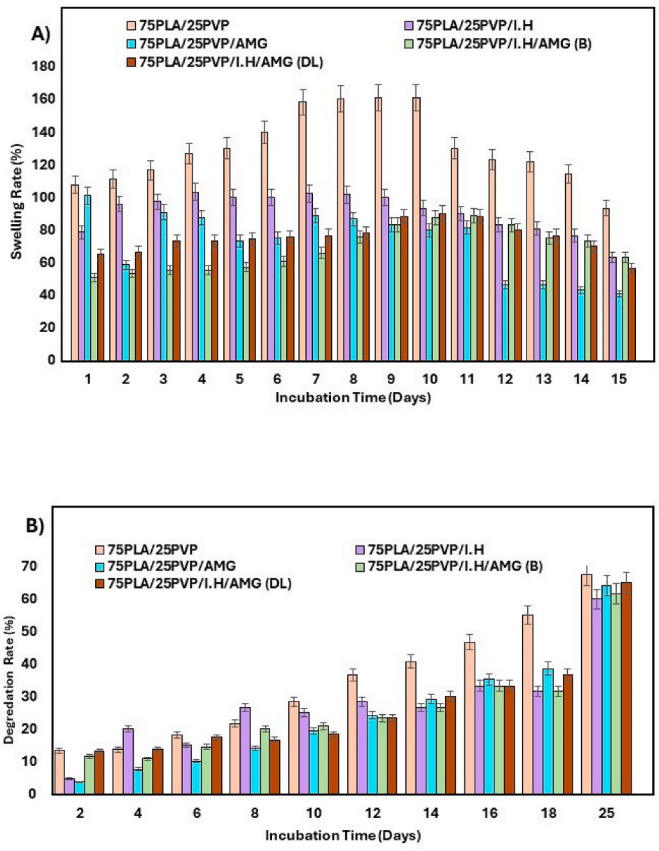

Fig. 6. Swelling (A) and degradation (B) graphs of nanofibrous patch.

cell adhesion, proliferation and growth [38,39]. In Fig. 6A, time-dependent swelling rates of fiber groups are given. For the swelling test, the swelling test was performed with PBS solution (pH: 7.4), which can best mimic the biological fluid of the human body, for 15 days, and the swelling performance of the nanofibrous samples was examined. According to the 15-day result, the 75PLA/25PVP group has the highest swelling rate, while there is no significant difference in the swelling rate of the other groups. According to the graph given in Fig. 6A, it is seen that the nanofiber fibers show swelling behavior until the 10th day. While the swelling rate on the 10th day was 161 % for 75PLA/25 PVP, on the same day, the 75PLA/25PVP/AMG loaded nanofiber fiber group had the least swelling profile with a rate of 80 %. At the end of 15 days, the group that absorbed the most water was 75PLA/25PVP with a rate of 93.33 %, while the group that absorbed the least water was 75PLA/25PVP/AMG with a rate of 41 %. It is known that nanofibrous with higher water absorbency degrade faster [40]. Therefore, in the 25-day period, the 75PLA/25PVP nanofibrous group may have degraded faster than the other groups because it absorbed more water. Due to the decrease in the swelling rate over time due to the deterioration of the hydrophilic component [41], the swelling rate of fibers containing PLA/PVP also decreased over time. Since the ratio of 75PLA and 25PVP is the same in all nanofibrous fibers, the swelling ratios are close to each other when the results are compared.

Degradability is an essential feature of biomaterials in tissue engineering studies. The scaffolds are expected to degrade over time after providing tissue regeneration [42]. Materials kept in PBS decompose over time and lose their mass during weighing. Also, after being kept in a humid environment, the ester groups in the main chain of PLA break down, and due to this breakdown, the molecular weight of PLA decreases [43,44]. According to Fig. 6B–as a result of monitoring the degradation of nanofibrous groups, the pure group consisting of 75PLA/25PVP is the group with the fastest degradation rate. The AMG drug-loaded group had the lowest degradation rate. At the end of 25 days, the 75PLA/25PVP group showed a degradation rate of 67.5 %, while the degradation rate of the other groups was as follows; 75PLA/25PVP/IH/AMG (DL), 75PLA/25PVP/AMG, 75PLA/25PVP/I-H/AMG (B), 75PLA/25PVP/IH; It is 65 %, 64.15 %, 61.66 %, 60 %. According to these results, it can be stated that I.H plant extract affects the degradation rate less than others. In the study of Mousa et al., it was observed that PLA nanofibrous used as hydrophobic polymers degraded roughly slowly [45]. Since PLA is a hydrophobic polymer, it takes a long time to degrade. In our nanofibrous structure, the proportion of PLA is 75 % and PVP is 25 %. Therefore, nanofibrous may have shown slow degradation behavior. In this study, the addition of *I.H* and AMG to the nanofibrous had a very slight effect on the swelling and degradation results.

3.7. In vitro drug release

In vitro drug release testing was performed to evaluate the drug release properties of *I.H* and AMG substances loaded into nanofibrous patches produced for the treatment of colon cancer. UV spectra were determined, and calibration curves were drawn. To equalise physiological conditions, releases were made in a medium containing PBS. The absorbance values for released AMG (R^2: 0.9997) and *I.H* (R^2: 0,9921) are UV 218 nm and 345 nm. It is seen that 72.27 % of the AMG-loaded

nanofibrous patch was released in the first 60 min in Fig. 7A (d). After the first hour, the release is on a slow and continuous slope. In the study conducted by Seyhan et al., it was seen that PLA/PEG nanofibrous loaded with different amounts of AMG drug showed a rapid drug release performance up to the first 90 min. It was observed that the AMG drug showed the typical two-step progression profile in a nanofibrous patch [1]. It was determined that the release of *I.H* loaded nanofibrous patch was 95.15 % in 24 h in Fig. 7B (d). This indicates a significant burst release phase. Post this initial burst release, the remaining drug was released in a more controlled and sustained manner, extending up to 180 h. This extended release phase, although slower, still contributes to the overall drug release profile, ensuring a prolonged therapeutic effect. In the study conducted by Chou et al., it was stated that as the diameter of the nanofibrous loaded with the drug increases, the release rate slows down. In the study, when large-diameter fibers and small-diameter fibers were compared, fibers with small diameters released the drug faster. Higher drug loading often results in increased burst release due to the more significant amounts of surface-associated drug and the higher surface area of the fibers [46]. Compared to the AMG drug, *I.H* provides a faster drug release result. When a comparison was made over the first hour, the *I.H*.-loaded fiber with a diameter of 525.34 nm released the drug at a higher rate than the AMG-loaded fiber with a diameter of 536.95 nm. Release studies have shown that larger diameter fibers release slower than smaller fibers. These differences in drug release as a function of fiber diameter may result from swelling behavior and drug solubility in different fiber formulations [47]. As reported in previous studies, faster diffusion or burst release can be observed for releasing small molecule drugs with hydrophilic properties [48]. As a result, the release of AMG and *I.H* from the nanofibrous patch took up to 180 h to complete. Studies have been conducted at various concentrations for both substances. In this study, optimum concentrations were determined and examined [1,3].

3.8. Cell culture test and MTT cytotoxicity assay

The effects of loaded with AMG and *I.H* in different shapes on cell viability were evaluated by MTT analysis for 1, 3, and 7 days in HCT-116 cell line. The main fiber material (75PLA/25PVP) produced in this

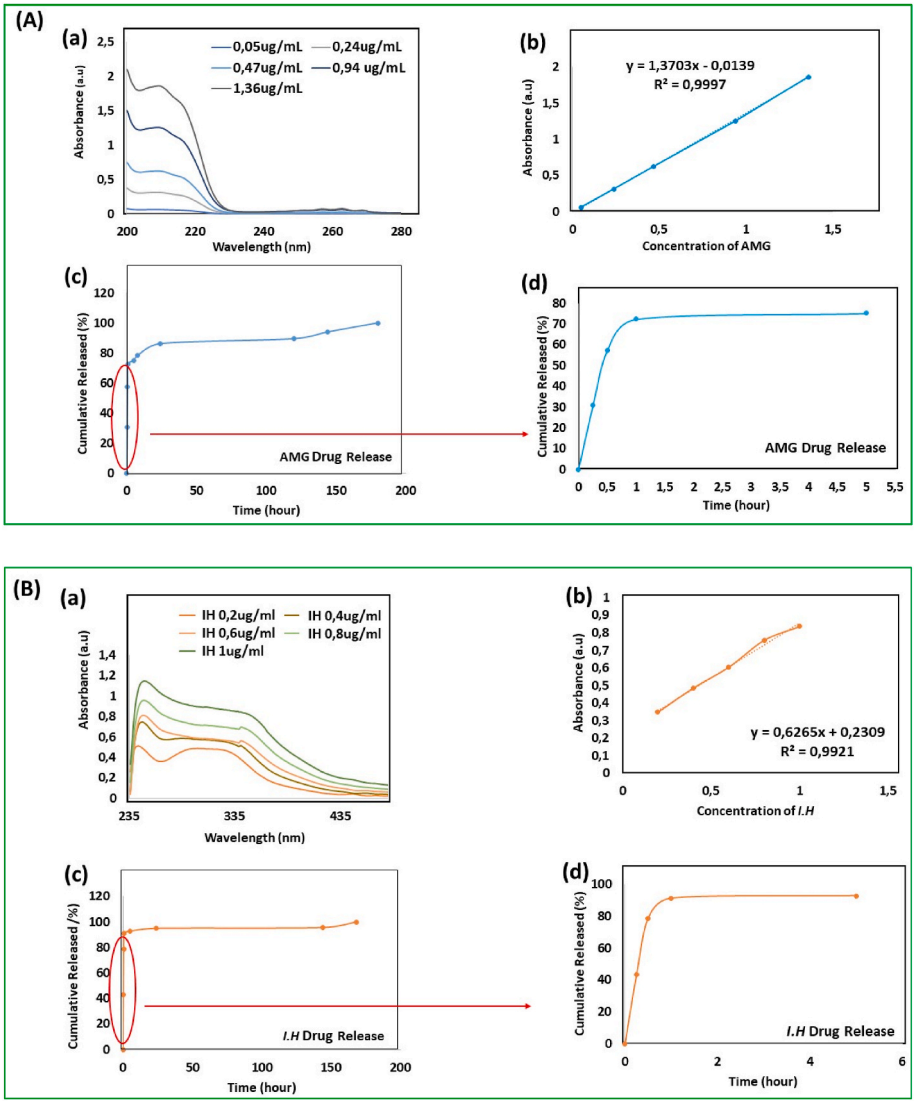

Fig. 7. In vitro drug release profiles of 75PLA/25PVP/AMG nanofibrous: Absorption spectra of AMG at different concentrations A (a), AMG calibration curve (b), cumulative drug release profiles from the 75PLA/25PVP/AMG electrospun nanofibrous between 0 and 5 h (c). Cumulative drug release from 75PLA/25PVP/AMG for 180 h (d) All the measurements were repeated three times, and the errors were less than 5 %, and in vitro drug release profiles of 75PLA/25PVP/*I.H* nanofibrous: Absorption spectra of *I.H* at different concentrations B (a), *I.H* calibration curve (b), cumulative drug release profiles from the 75PLA/25PVP/*I.H* electrospun nanofibrous between 0 and 5 h (c). Cumulative drug release from 75PLA/25PVP/*I.H* for 180 h (d). All the measurements were repeated three times, and the errors were less than 5 %.

study was reported to be non-toxic to the HCT-116 cells, compared to the control group (2D) for days 1, 3, and 7, respectively, are 95.24 %, 98.05 %, and 96.7 % in Fig. 8A. Cell viability was determined to be at significantly toxic levels in the main fiber material groups loaded with *I.H*, AMG and combined. When the results are examined, it can be stated that both AMG and *I.H.* materials loaded on nanofibrous patches give positive results in cancer cell death. Compared to AMG and I.H, AMG nanofibers gave a more effective result by showing less living cell behavior on the HCT-116 colon cancer cell line. The most significant reduction was in the 75PLA/25PVP/AMG group, loaded with AMG alone. The 3rd day was the day when the highest effect on the decrease of cell viability of AMG and *I.H* loaded fibers was observed. The group in which AMG and *I.H* were mixed and loaded on the fiber gave better results than those in which they were loaded separately in layers. Mixing

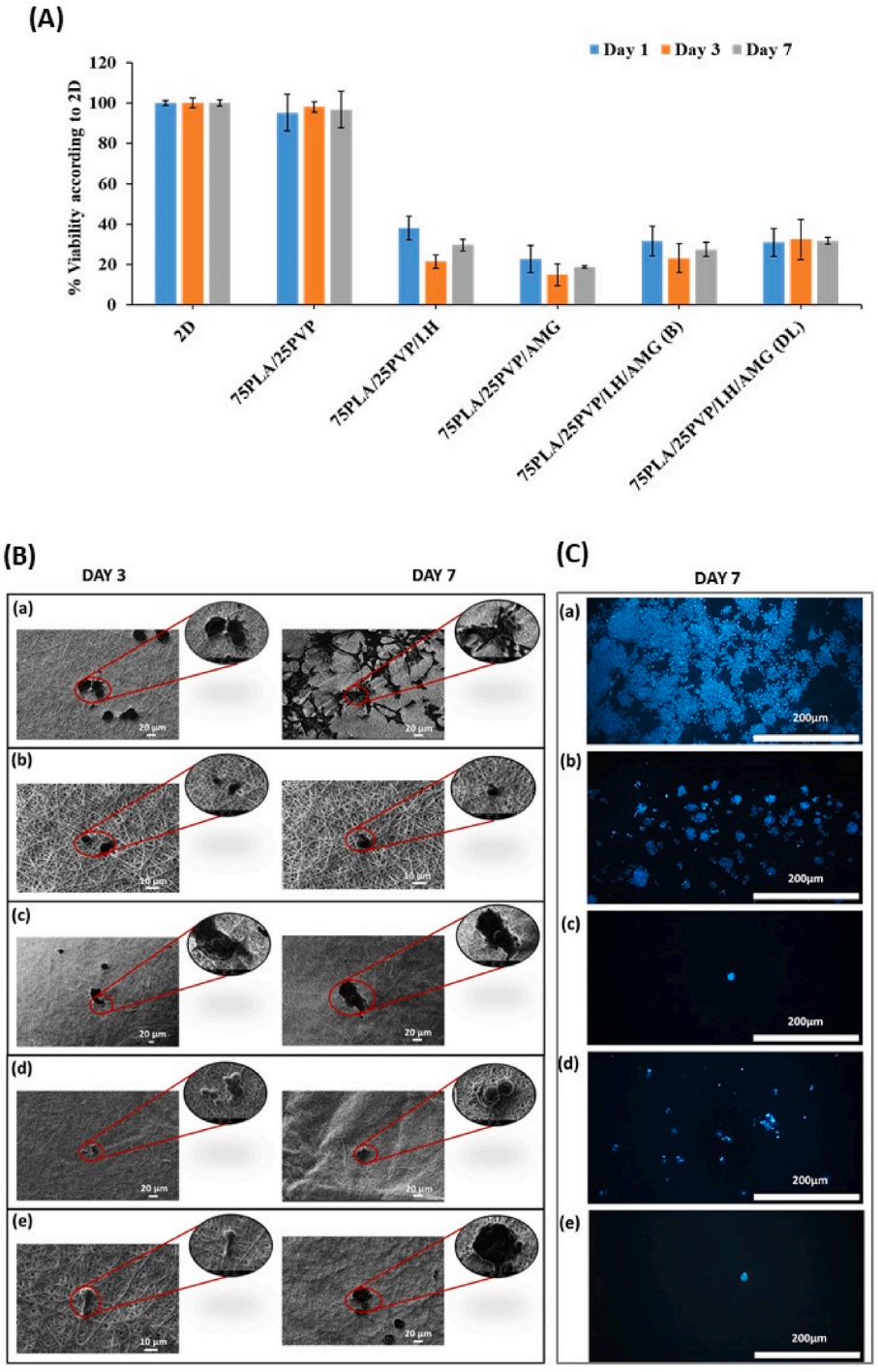

Fig. 8. Cell proliferation percentage of HCT-116 cells on A 75PLA/25PVP, 75PLA/25PVP/*I.H*, 75PLA/25PVP/AMG, 75PLA/25PVP/*I.H*/AMG (B) and 75PLA/25PVP/*I.H*/AMG (DL) nanofibrous patches on the 1st, 3rd, and 7th days (One-way Analysis of Variance (ANOVA) Turkey-Kramer Multiple Comparisons Test Comparison to 2D, **p < 0,01, ***p < 0,001). SEM images of the 1st and 3rd days of MTT tests of the nanofibrous patch. Images were 10 µm and 20 µm scale. The scale of the zoomed-in images was 2 µm and 10 µm. B(a) 75PLA/25PVP, (b) 75PLA/25PVP/*I.H*, (c) 75PLA/25PVP/AMG, (d) 75PLA/25PVP/*I.H*/AMG (B), and (e) 75PLA/25PVP/*I.H*/AMG (DL). Fluorescence images of the cells on the material on the 7th day. DAPI dye was used to obtain images. C(a) 75PLA/25PVP, (b) 75PLA/25PVP/*I.H*, (c) 75PLA/25PVP/AMG, (d) 75PLA/25PVP/*I.H*/AMG (B), and (e) 75PLA/25PVP/*I.H*/AMG (DL).

the active ingredients and loading the nanofibrous gave more successful results than the individual double-layer loading. In the study of Kyung-Nam et al., the effect of AMG on colon cancer was investigated. It has been proven that the drug AMG has a cytotoxic effect on colon cancer cells. This cytotoxic effect caused a decrease in cell viability due to the increase in drug concentration [49]. In their study, Dorn et al. tested the *I.H* extract on four tumor cell types: HT-29 (colon cancer), MCF-7 (breast cancer), Capan-2 (pancreatic cancer), and G1 (astrocytoma). Obtaining a highly toxic effect on all four tumor cell lines as a result of the MTT test, Dorn et al. demonstrated that *I.H* is an excellent candidate to be used in anticancer research. When the cells killed by *I.H* extract were examined under the electron microscope, the findings obtained such as irregular condensation of chromatin and ruptured swollen mitochondria in the images of HT-29 colon cancer cells showed parallel results with the MTT results [50].

Fluorescent images of the produced nanofibrous groups were examined by the DAPI staining method, one of the fluorescent techniques used in cell attachment detection in Fig. 8C, in which were demonstrated the biocompatibility of the produced fiber materials. In the fluorescence images, cell deaths have occurred, which may be due to reasons such as changes in the membrane integrity of the cells, loss of asymmetry of the cell membrane, and DNA fragmentation [51]. While the fluorescence intensity is lower in areas where cell death occurs, the intensity is higher in areas where live cells are present. The expected cell adhesion is present in the pure group, which contains no active ingredient and consists only of the polymer combination. The regions with the blue dye image showed more pronounced fluorescence due to the density and clustering of colon cancer cells. Adhesion showed little activity due to the effect of the active ingredients used in other groups.

According to the SEM image in Fig. 8B when we compared the nanofibrous group containing *I.H* with the group containing AMG drug among the fiber groups, the 75PLA/25PVP/AMG group containing AMG showed less binding. This can be explained by the effect of fiber-containing AMG drugs on cell death.

4. Conclusion

In this study, the electrospinning method successfully produced five different nanofibrous patch groups loaded with AMG and *I.H* for colon cancer treatment. Homogeneous distributed, bead-free nanofibrous images were obtained in the SEM results of AMG and *I.H* loaded fibers. In the mechanical strength test, the 75PLA/25PVP/*I.H*/AMG (DL) group showed less mechanical strength than the 75PLA/25PVP/*I.H*/AMG (B) group. When the drug release results were examined, it was seen that AMG and *I.H* loaded nanofibrous patches were released at a rate of 86.23 % and 95 %, respectively, at the end of 24 h. Both active substances were released for up to 180 h, and release was achieved. According to in-vitro cytotoxicity studies, all nanofibrous groups loaded with active ingredients showed cytotoxic effects against cancer cell lines. While the use of AMG and *I.H* alone showed a cytotoxic effect on the cell, importantly, their combined use also killed colon cancer cells. When we compare the combination types, it is possible to say that the blend combination gives better results than the DL combination. In the complex intestinal organ where cancer occurs, AMG and *I.H* loaded nanofibrous patches, which can be produced by electrospinning in sizes, geometric forms, and flexibility specific to the tumour area, can surgically cover and surround the wound. Therefore, the nanofibrous patch in this study may be a promising biomaterial that can be used in post-operative medical applications to reduce tumor tissues and initiate the process of healthy tissue regeneration in the treatment of colon cancer.

CRediT authorship contribution statement

Rabia Betul Sulutas: Writing – original draft, Investigation. **Sumeyye Cesur:** Writing – review & editing, Methodology, Conceptualization. **Serap Ayaz Seyhan:** Methodology, Investigation. **Dilek Bilgic Alkaya:** Visualization, Investigation. **Ali Sahin:** Methodology, Investigation. **Nazmi Ekren:** Methodology, Investigation. **Oguzhan Gunduz:** Writing – review & editing, Methodology.

Declaration of competing interest

The authors declare that they have no known competing financial interests or personal relationships that could have appeared to influence the work reported in this paper.

Data availability

The data that has been used is confidential.

Acknowledgements

The authors thanks to Marmara University Scientific Research Committee (Project Number: FYL-2024-11178) for their financial support.

References

[1] S.A. Seyhan, D.B. Alkaya, S. Cesur, A. Sahin, Investigation of the antitumor effect on breast cancer cells of the electrospun amygdalin-loaded poly(l-lactic acid)/poly (ethylene glycol) nanofibers, Int. J. Biol. Macromol. 239 (2023) 124201, https://doi.org/10.1016/J.IJBIOMAC.2023.124201.
[2] H.J. Park, S.H. Yoon, L.S. Han, L.T. Zheng, K.H. Jung, Y.K. Uhm, J.H. Lee, J. S. Jeong, W.S. Joo, S.V. Yim, J.H. Chung, S.P. Hong, Amygdalin inhibits genes related to cell cycle in SNU-C4 human colon cancer cells, World J. Gastroenterol. 11 (2005) 5156–5161.
[3] S. Cesur, Antioxidant and anti-tumour activities of inula viscosa L extract-loaded nanofibrous mats for biomedical applications, Ceram. - Silikaty. 67 (2023) 411–419, https://doi.org/10.13168/cs.2023.0041.
[4] J.E. Olguin, M.G. Mendoza-Rodriguez, C.A. Sanchez-Barrera, L.I. Terrazas, Is the combination of immunotherapy with conventional chemotherapy the key to increase the efficacy of colorectal cancer treatment? World J. Gastrointest. Oncol. 15 (2023) 251–267, https://doi.org/10.4251/wjgo.v15.i2.251.
[5] H. Yuan, Q. Ma, L. Ye, G. Piao, The traditional medicine and modern medicine from natural products, Molecules 21 (2016) 559, https://doi.org/10.3390/molecules21050559.
[6] C.A. Dehelean, I. Marcovici, C. Soica, M. Mioc, D. Coricovac, S. Iurciuc, O.M. Cretu, I. Pinzaru, Drug discovery and alternative therapy, Molecules 1096 (2021) 1–29.
[7] R. Arpita, Tushita Attre, Navneeta Bharadvaja, Anticancer agent from medicinal plants: a review, New Apects Med, Plants Pharmacogn 1 (2017) 54–73.
[8] E. Eroglu, S.N. Girgin, A unique phenolic extraction method from olive oil macerate of Hypericum perforatum using DMSO: assessment of in vitro anticancer activity, LC-MS/MS profile, total phenolic content and antioxidant capacity, South African J. Bot. 139 (2021) 6–11, https://doi.org/10.1016/j.sajb.2021.01.015.
[9] Y.Y. Yan, Q. Zhang, B. Zhang, B. Yang, N.M. Lin, Active ingredients of Inula helenium L. exhibits similar anti-cancer effects as isoalantolactone in pancreatic cancer cells, Nat. Prod. Res. 34 (2020) 2539–2544, https://doi.org/10.1080/14786419.2018.1543676.
[10] M.-K.J. Jaemoo Chun, Sang-Min Park, Minsung Lee, In Jin Ha, The sesquiterpene lactone-rich fraction of inula helenium L, Cancers (2023).
[11] M. Hayta, M. Alpaslan, Apricot kernel flour and its use in maintaining health, in: V. R. Preedy, R.R. Watson, V.B. Patel (Eds.), Flour Breads Their Fortif. Heal. Dis. Prev., Elsevier, San Diego, 2011, pp. 213–221, https://doi.org/10.1016/B978-0-12-380886-8.10020-0.
[12] P.K. Vemula, N.R. Campbell, F. Zhao, B. Xu, G. John, J.M. Karp, Self-assembled prodrugs, in: P. Ducheyne (Ed.), Compr. Biomater., Elsevier, Oxford, 2011, pp. 339–355, https://doi.org/10.1016/B978-0-08-055294-1.00135-5.
[13] G. Kalaiyarasan, M. Veerapandian, G. JebaMercy, K. Balamurugan, J. Joseph, Amygdalin-Functionalized carbon quantum dots for probing β-Glucosidase activity for cancer diagnosis and therapeutics, ACS Biomater. Sci. Eng. 5 (2019) 3089–3099, https://doi.org/10.1021/acsbiomaterials.9b00394.
[14] A.M. Alwan, D. Rokaya, G. Kathayat, J.T. Afshari, Onco-immunity and therapeutic application of amygdalin: a review, J. Oral Biol. Craniofacial Res. 13 (2023) 155–163, https://doi.org/10.1016/j.jobcr.2022.12.010.
[15] J. Shi, Q. Chen, M. Xu, Q. Xia, T. Zheng, J. Teng, M. Li, L. Fan, Recent updates and future perspectives about amygdalin as a potential anticancer agent: a review, Cancer Med. 8 (2019) 3004–3011, https://doi.org/10.1002/cam4.2197.
[16] S. Cesur, E. Ilhan, E. Pilavci, R.B. Sulutas, M. Gurboga, O. Bingol Ozakpinar, E. Kaya, M. Heljak, G. Bosgelmez Tinaz, F.N. Oktar, O. Gunduz, E. Kijeńska-Gawrońska, A novel strategy as a potential rapid therapy modality in the treatment of corneal ulcers: fluconazole/vancomycin dual drug-loaded nanofibrous patches, Macromol. Mater. Eng. 308 (2023), https://doi.org/10.1002/mame.202200697.
[17] N. Salahuddin, E.M. Ibrahim, M. El-Kemary, Electrospun composite nanofibers based on PLA/Artesunate-loaded citrate-functionalized hydroxyapatite for

boosting in vitro anticancer efficacy and drug delivery of artesunate, Fibers Polym. 23 (2022) 3415–3426, https://doi.org/10.1007/s12221-022-4017-3.
[18] W.J. Choi, K.S. Hwang, H.J. Kwon, C. Lee, C.H. Kim, T.H. Kim, S.W. Heo, J.-H. Kim, J.-Y. Lee, Rapid development of dual porous poly(lactic acid) foam using fused deposition modeling (FDM) 3D printing for medical scaffold application, Mater. Sci. Eng. C. 110 (2020) 110693, https://doi.org/10.1016/j.msec.2020.110693.
[19] H.Y. Cakmak, H. Ege, S. Yilmaz, G. Agturk, F.D. Yontem, G. Enguven, A. Sarmis, Z. Cakmak, O. Gunduz, Z.R. Ege, 3D printed Styrax Liquidus (Liquidambar orientalis Miller)-loaded poly (L-lactic acid)/chitosan based wound dressing material: fabrication, characterization, and biocompatibility results, Int. J. Biol. Macromol. 248 (2023) 125835, https://doi.org/10.1016/j.ijbiomac.2023.125835.
[20] E. Saylam, Y. Akkaya, E. Ilhan, S. Cesur, E. Guler, A. Sahin, M.E. Cam, N. Ekren, F. N. Oktar, O. Gunduz, D. Ficai, A. Ficai, Levodopa-loaded 3d-printed poly (Lactic) acid/chitosan neural tissue scaffold as a promising drug delivery system for the treatment of Parkinson's disease, Appl. Sci. 11 (2021), https://doi.org/10.3390/app112210727.
[21] S. Cesur, Combination techniques towards novel drug delivery systems manufacturing: 3D PCL scaffolds enriched with tetracycline-loaded PVP nanoparticles, Eur. J. Pharm. Biopharm. 194 (2024) 36–48, https://doi.org/10.1016/j.ejpb.2023.11.022.
[22] K. Nasouri, A.M. Shoushtari, M.R.M. Mojtahedi, Evaluation of effective electrospinning parameters controlling polyvinylpyrrolidone nanofibers surface morphology via response surface methodology, Fibers Polym. 16 (2015) 1941–1954, https://doi.org/10.1007/s12221-015-5263-4.
[23] D.B. Alkaya, S.A. Seyhan, B.N. Ozturk, Influence of extraction method on antioxidant properties of Rheum ribes root extract, Ovidius Univ. Ann. Chem. 30 (2019) 44–47, https://doi.org/10.2478/auoc-2019-0008.
[24] E. Ilhan, Z. Karahaliloglu, E. Kilicay, B. Hazer, E.B. Denkbas, Potent Bioactive Bone cements impregnated with polystyrene-g-soybean oil-AgNPs for advanced bone tissue applications, vol. 35, 2019, pp. 179–194, https://doi.org/10.1080/10667857.2019.1661157, 10.1080/10667857.2019.1661157.
[25] E. Ilhan, S. Cesur, R. Betul, E. Pilavci, B. Dalbayrak, The Role of Multilayer Electrospun Poly (Vinyl Alcohol)/Gelatin nanofibers loaded with Fluconazole and Cinnamaldehyde in the Potential Treatment of Fungal Keratitis, vol. 176, 2022, https://doi.org/10.1016/j.eurpolymj.2022.111390.
[26] R. Sridhar, S. Ravanan, J.R. Venugopal, S. Sundarrajan, D. Pliszka, S. Sivasubramanian, P. Gunasekaran, M. Prabhakaran, K. Madhaiyan, A. Sahayaraj, K.H.C. Lim, S. Ramakrishna, Curcumin-and natural extract-loaded nanofibres for potential treatment of lung and breast cancer: in vitro efficacy evaluation, J. Biomater. Sci. Polym. Ed. 25 (2014) 985–998, https://doi.org/10.1080/09205063.2014.917039.
[27] T. Fan, R. Daniels, Preparation and characterization of electrospun polylactic acid (PLA) fiber loaded with birch bark triterpene extract for wound dressing, AAPS PharmSciTech 22 (2021) 1–9, https://doi.org/10.1208/s12249-021-02081-z.
[28] S. Cesur, S. Ulag, L. Ozak, A. Gumussoy, S. Arslan, B.K. Yilmaz, N. Ekren, M. Agirbasli, D.M. kalaskar, O. Gunduz, Production and characterization of elastomeric cardiac tissue-like patches for Myocardial Tissue Engineering, Polym. Test. 90 (2020) 106613, https://doi.org/10.1016/j.polymertesting.2020.106613.
[29] A.M. Abdelghany, M.S. Mekhail, E.M. Abdelrazek, M.M. Aboud, Combined DFT/FTIR structural studies of monodispersed PVP/Gold and silver nano particles, J. Alloys Compd. 646 (2015) 326–332, https://doi.org/10.1016/j.jallcom.2015.05.262.
[30] R. Sohail, S.R. Abbas, Evaluation of amygdalin-loaded alginate-chitosan nanoparticles as biocompatible drug delivery carriers for anticancerous efficacy, Int. J. Biol. Macromol. 153 (2020) 36–45, https://doi.org/10.1016/j.ijbiomac.2020.02.191.
[31] E. Ahmadi, M.M. Farimani, H. Rezadoost, Optimization of inulin extraction from Inula helenium L. using response surface methodology followed by its MALDI-TOF and TLC-FLD based characterization, J. Med. Plants. 21 (2022) 43–55, https://doi.org/10.52547/jmp.21.82.43.
[32] M.E. Cam, A.N. Hazar-Yavuz, S. Cesur, O. Ozkan, H. Alenezi, H. Turkoglu Sasmazel, M. Sayip Eroglu, F. Brako, J. Ahmed, L. Kabasakal, G. Ren, O. Gunduz, M. Edirisinghe, A novel treatment strategy for preterm birth: intra-vaginal progesterone-loaded fibrous patches, Int. J. Pharm. 588 (2020) 119782, https://doi.org/10.1016/j.ijpharm.2020.119782.
[33] Ö. Aybastıer, Efficacy of methanol-water extract of Inula helenium root against oxidative DNA damage, J. Tradit. Chinese Med. 41 (2021) 293–300, https://doi.org/10.19852/j.cnki.jtcm.20210209.008.
[34] N. Petkova, I. Ivanov, R. Vrancheva, P. Denev, A. Pavlov, Ultrasound and microwave-assisted extraction of elecampane (Inula helenium) roots, Nat. Prod. Commun. 12 (2017) 171–174, https://doi.org/10.1177/1934578x1701200207.
[35] A. Gökbulut, O. Özhan, B. Satilmis, K. Batçioglu, S. Günal, E. Şarer, Antioxidant and antimicrobial activities, and phenolic compounds of selected inula species from Turkey, Nat. Prod. Commun. 8 (2013) 475–478, https://doi.org/10.1177/1934578x1300800417.
[36] Z. Stojanović-Radić, L. Čomić, N. Radulović, P. Blagojević, M. Denić, A. Miltojević, J. Rajković, T. Mihajilov-Krstev, Antistaphylococcal activity of Inula helenium L. root essential oil: eudesmane sesquiterpene lactones induce cell membrane damage, Eur. J. Clin. Microbiol. Infect. Dis. 31 (2012) 1015–1025, https://doi.org/10.1007/s10096-011-1400-1.
[37] S. Cesur, E. Ilhan, T.A. Tut, E. Kaya, B. Dalbayrak, G. Bosgelmez-Tinaz, E.D. Arısan, O. Gunduz, E. Kijeńska-Gawrońska, Design of cinnamaldehyde- and gentamicin-loaded double-layer corneal nanofiber patches with antibiofilm and antimicrobial effects, ACS Omega (2023), https://doi.org/10.1021/acsomega.3c00914.
[38] W. Cui, X. Li, S. Zhou, J. Weng, Degradation patterns and surface wettability of electrospun fibrous mats, Polym. Degrad. Stab. 93 (2008) 731–738, https://doi.org/10.1016/j.polymdegradstab.2007.12.002.
[39] R. Nirmala, H.-M. Park, R. Navamathavan, H.-S. Kang, M.H. El-Newehy, H.Y. Kim, Lecithin blended polyamide-6 high aspect ratio nanofiber scaffolds via electrospinning for human osteoblast cell culture, Mater. Sci. Eng. C. 31 (2011) 486–493, https://doi.org/10.1016/j.msec.2010.11.013.
[40] D. Wang, D.J.T. Hill, H. Peng, A. Symons, S. Varanasi, A.K. Whittaker, F. Rasoul, Development of injectable biodegradable multi-arms PEG-based hydrogels: swelling and degradation investigations, Macromol. Symp. 296 (2010) 233–237, https://doi.org/10.1002/masy.201051033.
[41] M. Hadjianfar, D. Semnani, J. Varshosaz, Polycaprolactone/chitosan blend nanofibers loaded by 5-fluorouracil: an approach to anticancer drug delivery system, Polym. Adv. Technol. 29 (2018) 2972–2981, https://doi.org/10.1002/pat.4417.
[42] J.P. Martins, M.P.A. Ferreira, N.Z. Ezazi, J.T. Hirvonen, H.A. Santos, G. Thrivikraman, C.M. França, A. Athirasala, A. Tahayeri, L.E. Bertassoni, 3D printing: prospects and challenges, in: Nanotechnologies Prev. Regen. Med., Elsevier, 2018, pp. 299–379, https://doi.org/10.1016/B978-0-323-48063-5.00004-6.
[43] E. Ilhan, S. Cesur, E. Guler, F. Topal, D. Albayrak, M.M. Guncu, M.E. Cam, T. Taskin, H.T. Sasmazel, B. Aksu, F.N. Oktar, O. Gunduz, Development of Satureja cuneifolia-loaded sodium alginate/polyethylene glycol scaffolds produced by 3D-printing technology as a diabetic wound dressing material, Int. J. Biol. Macromol. 161 (2020) 1040–1054, https://doi.org/10.1016/j.ijbiomac.2020.06.086.
[44] N.F. Zaaba, M. Jaafar, A review on degradation mechanisms of polylactic acid: hydrolytic, photodegradative, microbial, and enzymatic degradation, Polym. Eng. Sci. 60 (2020) 2061–2075, https://doi.org/10.1002/pen.25511.
[45] H.M. Mousa, M.G. Ali, A.I. Rezk, E.A. Nasr, K.H. Hussein, Development of conductive polymeric nanofiber patches for cardiac tissue engineering application, J. Appl. Polym. Sci. 139 (2022) 1–17, https://doi.org/10.1002/app.52757.
[46] S.-F. Chou, D. Carson, K.A. Woodrow, Current strategies for sustaining drug release from electrospun nanofibers, J. Control. Release. 220 (2015) 584–591, https://doi.org/10.1016/j.jconrel.2015.09.008.
[47] G. Buschle-Diller, J. Cooper, Z. Xie, Y. Wu, J. Waldrup, X. Ren, Release of antibiotics from electrospun bicomponent fibers, Cellulose 14 (2007) 553–562, https://doi.org/10.1007/s10570-007-9183-3.
[48] S. Sena, K.N. Sumeyra, G. Ulkugul, A. Sema, K. Betul, S.B. Muge, E.M. Sayip, U. Muhammet, K. Cevriye, M. Mahir, M.A. Titu, D. Ficai, A. Ficai, O. Gunduz, Controlled release of metformin hydrochloride from core-shell nanofibers with fish sarcoplasmic protein, Medicina (B. Aires). 55 (2019) 682, https://doi.org/10.3390/medicina55100682.
[49] K. Kim, Y. Song, H. Lim, Amygdalin Extract from Armeniacae Semen Induces Apoptosis in Human COLO 201 Colon Cancer Cells, 2005, p. 26.
[50] D.C. Dorn, M. Alexenizer, J.G. Hengstler, A. Dorn, Tumor cell specific toxicity of Inula helenium extracts, Phyther. Res. 20 (2006) 970–980, https://doi.org/10.1002/ptr.1991.
[51] M. Leite, M. Quinta-Costa, P.S. Leite, J.E. Guimarães, Critical evaluation of techniques to detect and measure cell death - study in a model of UV radiation of the leukaemic cell line HL60, Anal. Cell Pathol. 19 (1999) 139–151, https://doi.org/10.1155/1999/176515.